



## Electrochemically assisted photocatalytic degradation of oxalic acid on particulate TiO<sub>2</sub> film in a batch mode plate photoreactor

J. KRÝSA<sup>1\*</sup> and J. JIRKOVSKÝ<sup>2</sup>

<sup>1</sup>Institute of Chemical Technology, Department of Inorganic Technology, Technická 5, 166 28 Prague 6, Czech Republic

<sup>2</sup>J. Heyrovský Institute of Physical Chemistry, Academy of Sciences of the Czech Republic, Dolejškova 3, 182 23 Prague 8, Czech Republic

(\*author for correspondence)

Received 17 July 2001; accepted in revised form 19 February 2002

**Key words:** degradation, electrochemical, oxalic acid, particulate TiO<sub>2</sub>, photocatalytic

### Abstract

Electrochemically assisted photocatalytic degradation of oxalic acid was studied in a batch mode plate photoreactor composed of particulate TiO<sub>2</sub> film immobilized on Ti metal plate (Ti/TiO<sub>2</sub> electrode) and Pt wires immersed in a flowing film of aqueous solution (Pt counter electrode). The degradation rate of oxalic acid was followed as a function of the potential of the Ti/TiO<sub>2</sub> electrode, the oxygen concentration and the light intensity. The presence of oxalic acid caused an increase in the measured photocurrent by one order of magnitude which is due to its reaction with photogenerated holes. The degradation rate increased with increasing potential up to 0.5 V vs SCE, then the increase was more gradual. Electrochemically assisted photocatalytic degradation of oxalic acid also proceeded in the absence of oxygen. The photogenerated electrons caused hydrogen evolution (low oxygen concentration) or predominantly oxygen reduction (high oxygen concentration) on the Pt counter electrode.

### 1. Introduction

Photocatalysis on TiO<sub>2</sub> represents a newly developed alternative technology for degradation of organic pollutants and inactivation of microorganisms in water. It is based on photogeneration of separated electrons and positive holes in the semiconductor particles. These charge carriers either recombine inside the particle or move to its surface where they can react with adsorbed molecules. Positive holes typically oxidize organic compounds thus initiating their further oxidative degradation while electrons mainly reduce dioxygen producing superoxide radical anions. Recombination of photogenerated positive holes and electrons inside the semiconductor particles is generally responsible for a relatively low quantum yield of the photocatalytic degradation. A possible way of increasing the electron hole separation and, consequently, of enhancing quantum yield is the application of a potential bias.

The concept of achieving charge separation in semiconductor systems with an electrochemical bias was first introduced by Honda and Fujishima [1]. For a compact semiconductor (e.g., a single crystal) a depletion layer will be formed, normally depicted as band bending. The generation of a depletion layer requires the transfer of mobile charge carriers between the semiconductor and the electrolyte. When an electroactive species is present in the electrolyte the charge transfer can take place directly

across the semiconductor solution interface. Alternatively in the absence of a suitable redox couple in the solution, the semiconductor can be polarized by applying an external bias voltage across the junction via an ohmic contact mounted at the back of the electrode [2].

In photocatalytic degradation of pollutants the use of nanocrystalline semiconductor films is especially convenient due to its porous structure resulting in a large surface area. Two processing routes have been reported in the literature. In the first approach, nanocrystalline particles are formed directly onto the conductive support by electrochemical or chemical deposition processes [3–10]. In the second approach, nanocrystalline particles sediment to a conducting substrate from a suspension, forming nanoporous film. Sintering at 350–450 °C results in an electronic contact between the particles allowing charge transport to the support. Using the second-method we obtain a *particulate* film with highly porous structure [11–14]. Vinodgopal et al. [11] used a particulate film prepared by applying TiO<sub>2</sub> P25 slurry on conducting glass and sintering at 400 °C. Byrne et al. [13, 14] used electrophoretic coating of a Ti alloy substrate applying suspension of TiO<sub>2</sub> P25 in methanol and annealing at 500 °C. TiO<sub>2</sub> P25 (Degussa) is a nonporous 70:30% anatase-to-rutile mixture with a BET surface area of 55 ± 12 m<sup>2</sup> g<sup>-1</sup> and crystalline sizes of 30 nm in 0.1 μm diameter aggregates. The small particle size (such as found in Degussa P25) precludes

the formation of a depletion layer as such across the particle, and so the observed photoelectrochemistry is determined by the relative rates of capture of holes and electrons at the surface of the particles. An effect of electrode potential under these conditions can be ascribed to electrophoretic drift of electrons to the back contact of the photoanode. Thus one can minimize charge recombination by application of an anodic bias to the  $\text{TiO}_2$  film. Application of this simple logic of achieving better charge separation in particles is important for improving the efficiency of photocatalytic degradation of organic contaminants, partially offsetting the mass transfer problems connected with the use of semiconductor thin films.

This work is a continuation of previous studies [15–17] devoted to the photocatalytic degradation of oxalic acid on a *particulate*  $\text{TiO}_2$  layer (dip coating from suspension of  $\text{TiO}_2$  P25 on a glass support) in a batch mode plate photoreactor with a flowing film of aqueous solution. The present paper describes an electrochemically assisted photocatalytic degradation of oxalic acid on a *particulate*  $\text{TiO}_2$  layer prepared on a titanium metal plate. The influence of oxygen concentration, applied potential and light intensity on the degradation rate was investigated.

## 2. Experimental details

A batch mode plate photoreactor was employed with a flowing film of aqueous solution (thickness about 1 mm), irradiated by 1, 3 or 7 ultraviolet sun bed tubes (Osram Eversun L40W/79K) emitting wavelengths between 320 and 380 nm (maximum at 355 nm) (Figure 1). As a photocatalyst,  $\text{TiO}_2$  P25 (Degussa) was used. A particulate  $\text{TiO}_2$  layer was prepared on a titanium metal plate (length 60 cm, width 30 cm) by sedimentation from an aqueous suspension of  $\text{TiO}_2$  ( $10 \text{ g dm}^{-3}$ ) with subsequent drying and annealing at  $300^\circ\text{C}$ .

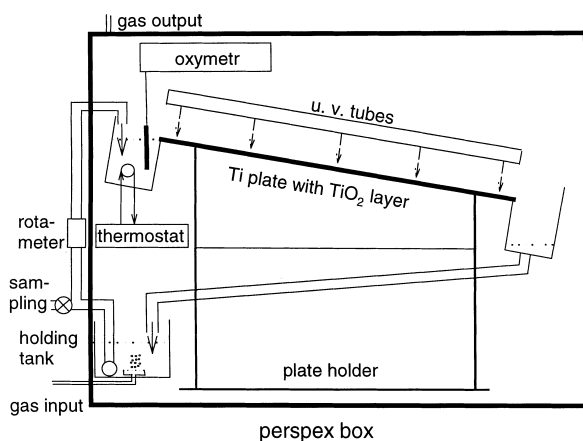


Fig. 1. Schematic representation of a batch mode plate reactor with flowing film of aqueous solution, Ti plate with  $\text{TiO}_2$  layer—width 300 mm, length 600 mm; inclination angle  $10^\circ$ ; distance between u.v. tubes and  $\text{TiO}_2$  layer 125 mm.

The solution of oxalic acid (initial concentration  $5 \text{ mol m}^{-3}$ ) was pumped from the four litre holding tank employing a centrifugal pump (Nova, Sicce, Italy) to the higher trough. The overflow produced a liquid film flowing over the glass plate fixed in the trays. The solution was collected in the lower trough and returned to the holding tank. The flow rate was controlled by rotameter.

The counter electrode consisted of 30 Pt wires (dia. 0.2 mm) immersed in the flowing aqueous film (Figure 2(a)) and placed in parallel with the flow so as not to disturb the laminar flow of the solution. The wire diameter was small (0.2 mm) in order to cause minimal losses of irradiated light. The distance between the parallel Pt wires was 1 cm and the spacing from the  $\text{TiO}_2$  electrode was about 0.5–1 mm.

The electrical circuit consisting of a d.c. power supply with voltage regulator, two high impedance voltmeters and an ammeter is shown in Figure 2(b). External voltage was applied between the Ti/ $\text{TiO}_2$  electrode and the Pt counter electrode because any practical system would almost certainly involve a two-electrode, rather than a three electrode system. The potentials of  $\text{TiO}_2$  and Pt electrode were measured against SCE.

The photoreactor was placed in a closed box that offered the possibility of controlling the composition of the internal atmosphere and thus adjusting various concentrations of oxygen in the aqueous oxalic acid solution. The oxygen concentration was adjusted by using different atmospheres (oxygen, nitrogen and a mixture) and measured using an oxymeter Multiline P4 with a Cellox 325 oxygen electrode (both products of WTW, Germany).

To follow the degradation kinetics, samples of the reaction mixture were taken at various appropriate irradiation times. The concentration of oxalic acid was determined by titration with potassium permanganate.

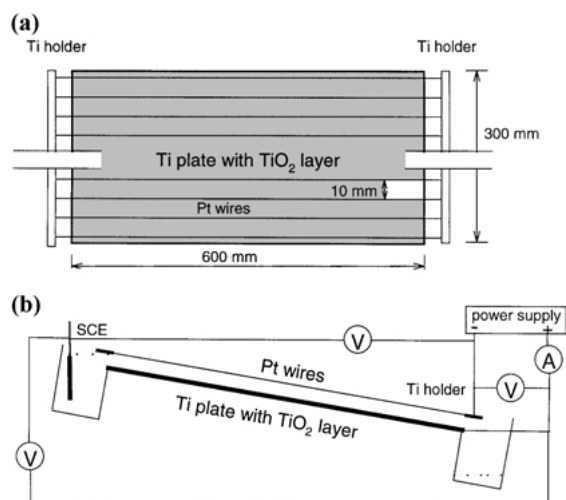


Fig. 2. (a) Detail of Pt counter electrode (top view). Diameter of Pt wires 0.2 mm; distance between parallel Pt wires was 1 cm and the spacing from  $\text{TiO}_2$  electrode was about 0.5–1 mm. (b) Electrical circuit and schema of electrodes arrangement (side view).

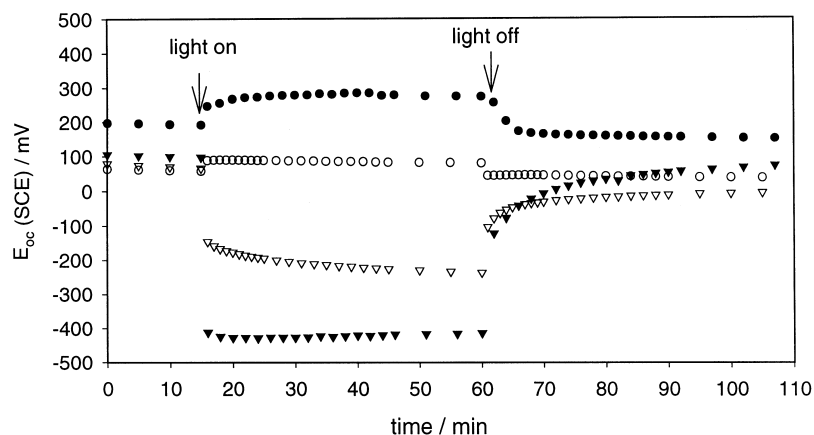


Fig. 3. Potential of (triangles)  $\text{TiO}_2/\text{Ti}$  electrode and (circles) Pt counter electrode against SCE either upon illumination or in dark in both (open symbols) absence and (solid symbols) presence of 0.005 M oxalic acid; electrolyte 0.1 M  $\text{NaClO}_4$ ,  $J_{hv} = 10.2 \times 10^{-5}$  einstein  $\text{m}^{-2} \text{s}^{-1}$ , flow rate  $150 \text{ dm}^3 \text{ h}^{-1}$ , oxygen concentration  $6.9 \text{ mg dm}^3$ .

### 3. Results

#### 3.1. Open circuit potential behaviour

The time dependence of the open circuit potential ( $E_{oc}$ ) is shown in Figure 3 (open symbols) for both  $\text{Ti}/\text{TiO}_2$  and Pt electrodes either during illumination or in dark, using 0.1 M  $\text{NaClO}_4$  as electrolyte. During the dark period, both  $\text{Ti}/\text{TiO}_2$  and Pt electrodes had potentials of approximately 60 mV and 65 mV vs SCE, respectively. Upon illumination, the potential of the  $\text{Ti}/\text{TiO}_2$  electrode jumped negatively to about  $-150$  mV and reached, during a further 60 min, a steady-state value of  $-240$  mV vs SCE. In contrast, the potential of the Pt electrode increased slightly after illumination (by about 15 mV). This could be attributed to the presence of small amounts of oxidative species formed on the illuminated  $\text{TiO}_2$  surface by the charge transfer reactions. When the light was switched off, the potential of the  $\text{Ti}/\text{TiO}_2$  electrode was slowly increased and reached its dark value within about 1 hour. An analogous effect was observed for the Pt electrode but its potential decreased very rapidly (during 1–2 min).

A similar course of the open circuit potential was observed when oxalic acid was added to the electrolyte solution (Figure 3, solid symbols). However, some differences were found as compared to the previous case of the pure electrolyte without oxalic acid. The potential decrease of the  $\text{Ti}/\text{TiO}_2$  electrode upon illumination was more rapid, and its steady state value was more negative by about  $-165$  mV. The potential increase of the Pt electrode upon illumination was also higher (by about 180 mV). The potential of both the  $\text{Ti}/\text{TiO}_2$  and Pt electrode decayed slowly when the illumination was stopped. It took about 1 h and 10 min, respectively. The decrease in potential of the  $\text{Ti}/\text{TiO}_2$  electrode upon illumination is due to the fact that photogenerated holes react fast on the surface and photogenerated electrons accumulate on the  $\text{TiO}_2$  surface and charge it negatively.

The degradation of oxalic acid under open circuit conditions for various oxygen concentrations is shown in Figure 4. The oxygen concentration was adjusted by setting the  $\text{N}_2$  to  $\text{O}_2$  ratio of the gas phase inside the closed box, which contained the whole photoreactor. All three time dependences shown in Figure 4 are almost linear corresponding to zero order kinetics of the degradation of oxalic acid. Its degradation flux was calculated by Equation 1 using the initial slopes of the kinetic dependencies, the overall volume of reaction mixture ( $V_r = 5 \text{ dm}^3$ ) and the geometrical area of illuminated photocatalyst layer ( $A = 18 \text{ dm}^2$ ). Considering the three limiting cases [15–17] the linear dependence of oxalic acid concentration on irradiation time means that the reaction rate was not controlled by the diffusion of oxalic acid to the  $\text{TiO}_2$  layer but by the flux of either oxygen or photons.

$$-|J_{(\text{COOH})_2}| = \left(\frac{V_r}{A}\right) \times \frac{d_{\text{c}(\text{COOH})_2}}{d\tau} \quad (1)$$

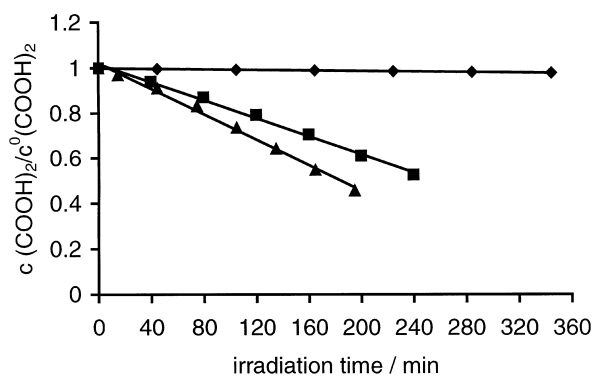


Fig. 4. Dependence of relative concentration of oxalic acid on irradiation time for three different bulk concentrations of oxygen ( $\blacklozenge$ ) 0.006, ( $\blacksquare$ ) 6.7 and ( $\blacktriangle$ )  $27.9 \text{ mg dm}^{-3}$  under open circuit conditions; electrolyte 0.1 M  $\text{NaClO}_4$ ,  $J_{hv} = 10.2 \times 10^{-5}$  einstein  $\text{m}^{-2} \text{s}^{-1}$ , flow rate  $150 \text{ dm}^3 \text{ h}^{-1}$ , initial concentration of oxalic acid was 0.005 M.

Table 1. Potentials of the Ti/TiO<sub>2</sub> electrode and degradation flux densities of oxalic acid,  $J_{(\text{COOH})_2}$ , for different bulk concentrations of oxygen for experiments at open circuit conditions

Conc. O <sub>2</sub> /mg dm <sup>-3</sup>	$E_{\text{Ti/TiO}_2}$ (SCE) /V	$J_{(\text{COOH})_2}$ /10 <sup>-6</sup> mol m <sup>-2</sup> s <sup>-1</sup>
27.9	-0.39	-6.17
6.7	-0.478	-4.51
0.006	-0.62	-0.18

The resulting values are summarized in Table 1. The degradation of oxalic acid proceeded very slowly at the lowest concentration of oxygen (about 0.006 mg dm<sup>-3</sup>) while it was almost 50 times faster for the highest oxygen concentration (27.9 mg dm<sup>-3</sup>). This confirmed the essential role of oxygen as a scavenger of photogenerated electrons.

The potential of the Ti/TiO<sub>2</sub> electrode depended on the concentration of oxygen. For its lower concentration, the consumption of electrons was slow; they accumulated on TiO<sub>2</sub> particles causing a negative potential shift. In the case of higher concentrations of oxygen, the electrons were consumed faster; their photostationary concentration on the TiO<sub>2</sub> layer was lower and the potential of the Ti/TiO<sub>2</sub> electrode increased.

### 3.2. Photocurrent–potential dependence

Current–potential dependences were measured for three different bulk concentrations of oxygen and in either the absence or presence of oxalic acid in solution. The results are shown in Figure 5. Practically no current flowed between the Ti/TiO<sub>2</sub> and Pt electrodes in dark, independently of the presence of oxalic acid. Upon illumination, a small increase in the oxidative current occurred for the pure electrolyte 0.1 M NaClO<sub>4</sub>. After addition of oxalic acid, the photocurrent increased by one order of magnitude. It had been previously reported [18] that oxalic acid gives rise to a pH-independent

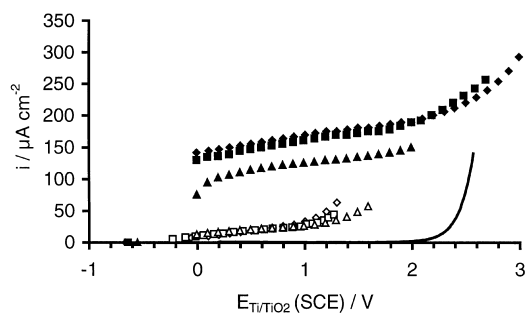


Fig. 5. Photocurrent–potential dependences for photoreactor with Ti/TiO<sub>2</sub> electrode and Pt counter electrode for three different bulk concentrations of oxygen. Dark (—), light, in the absence of oxalic acid: (◇) 0.055, (□) 7.1 and (△) 30.1 mg dm<sup>-3</sup>; light, in the presence of 0.005 M oxalic acid: (◆) 0.055, (■) 7.1 and (▲) 30.1 mg dm<sup>-3</sup>; electrolyte 0.1 M NaClO<sub>4</sub>,  $J_{hv} = 10.2 \times 10^{-5}$  einstein m<sup>-2</sup>s<sup>-1</sup>, flow rate 150 dm<sup>3</sup> h<sup>-1</sup>.

Table 2. Current densities for illuminated Ti/TiO<sub>2</sub> electrode at potential 1 V vs (SCE) in both absence and presence of oxalic acid and for different concentrations of oxygen

O <sub>2</sub> conc. /mg dm <sup>-3</sup>	Current density/10 <sup>-6</sup> A cm <sup>-2</sup>	
	NaClO <sub>4</sub>	NaClO <sub>4</sub> + (COOH) <sub>2</sub>
0.055	33.6	169
7.1	29.4	161
30.1	28.6	126

oxidation peak at pyrolytic graphite ( $E_p = 0.99$  V vs SCE) in acetate buffer. No oxidation peak was observed using a Pt working electrode in perchlorate as a supporting electrolyte [13]. The observed constant level of photocurrent (0–1.5 V) is due to the reaction of oxalic acid with photogenerated holes. Further increase in current for potentials higher than 1.5 V can be attributed to oxygen evolution which proceeds even in dark.

The values of the photocurrent at 1 V for different concentrations of oxygen are given in Table 2. It is apparent that the photocurrent decreased with increasing oxygen concentration. Vinodgopal et al. [11] reported similar observations. Applying bias to a thin particulate TiO<sub>2</sub> film it is generally difficult to achieve a total separation of positive holes and electrons. Therefore electrons are partly trapped on the TiO<sub>2</sub> surface and can react with oxygen. The efficiency of the electron transport via the external circuit from the illuminated Ti/TiO<sub>2</sub> electrode to the Pt counter electrode (i.e., the measured photocurrent) decreased with increasing oxygen concentration.

### 3.3. Effect of external voltage on degradation rate

The effect of external voltage, applied between the Ti/TiO<sub>2</sub> electrode and the Pt counter electrode, on the degradation rate of oxalic acid was investigated for three different light intensities and one oxygen concentration of 6.7 mg dm<sup>-3</sup> applying a flow rate of 2.5 dm<sup>3</sup> min<sup>-1</sup>. The potential of both Ti/TiO<sub>2</sub> and Pt electrode vs SCE was measured during each degradation experiment. The dependences of the degradation rate of oxalic acid on the Ti/TiO<sub>2</sub> potential (SCE) are shown in Figure 6 together with the data of open circuit experiments.

An obvious positive effect of increasing light intensity on increase in the degradation rate of oxalic acid can be seen. The values of  $E_{oc}$ , that is, of potential of the TiO<sub>2</sub> electrode under open circuit conditions, decreased with increasing light intensity. This was probably caused by the increasing number of positive holes and electrons photogenerated at higher light intensities. Positive holes reacted fast; electrons remained longer on the TiO<sub>2</sub> surface and charged it negatively. This negative charge was greater at higher light intensities corresponding to a higher photostationary number of accumulated electrons.

It can be further seen in Figure 6 that the obvious positive effect of the light intensity on the degradation

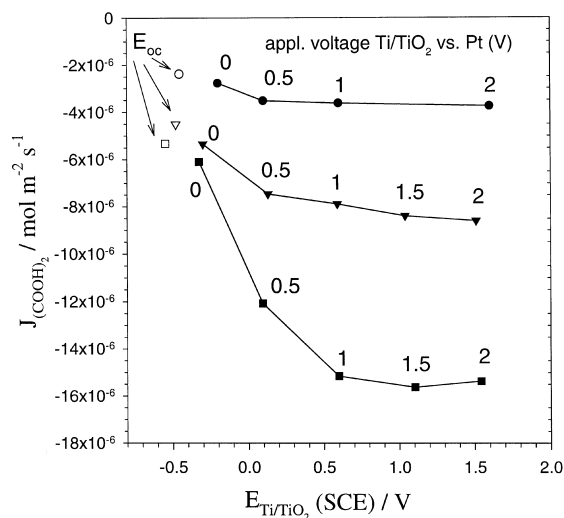


Fig. 6. Dependence of degradation rate of oxalic acid on Ti/TiO<sub>2</sub> potential (SCE) for three different photon flux intensities (●)  $3.5 \times 10^{-5}$ , (▼)  $10.2 \times 10^{-5}$  and (■)  $24.4 \times 10^{-5}$  einstein  $\text{m}^{-2} \text{s}^{-1}$  (open symbols correspond to open circuit conditions); oxygen concentration  $6.7 \text{ mg dm}^{-3}$ , electrolyte  $0.1 \text{ M NaClO}_4$ , flow rate  $150 \text{ dm}^3 \text{ h}^{-1}$ , initial concentration of oxalic acid was  $0.005 \text{ M}$ .

rate of oxalic acid varies considerably with the value of the applied voltage. For the bias voltage  $0 \text{ V}$ , change in the light intensity from  $10.2 \times 10^{-5}$  to  $2.44 \times 10^{-5}$  einstein  $\text{m}^{-2} \text{s}^{-1}$  caused an increase in the degradation rate by only 14%, and for the bias  $1 \text{ V}$  by 92%. As already stated, application of the positive potential bias to the particulate TiO<sub>2</sub>/Ti electrode provides a potential gradient within the semiconductor layer to drive the photogenerated holes and electrons efficiently apart. As a result, the charge recombination is reduced, and, consequently, a higher amount of positive holes is available for the photooxidation of oxalic acid. The greatest increase in degradation rate was observed for the bias voltage  $0.5$  and  $1 \text{ V}$  ( $E_{\text{TiO}_2}$  from  $-0.3$  to  $0.5 \text{ V}$  vs SCE). This is consistent with the observed increase in photocurrent between  $0$  and  $1 \text{ V}$  vs SCE (Figure 5). For higher voltages no further increase in reaction rate was achieved.

The effect of voltage bias increased with increasing light intensity. Applying  $1 \text{ V}$ , the degradation rate increased, compared to open circuit conditions, by only 50% for  $3.5 \times 10^{-5}$  einstein  $\text{m}^{-2} \text{s}^{-1}$ , and by 180% for  $24.4 \times 10^{-5}$  einstein  $\text{m}^{-2} \text{s}^{-1}$ .

### 3.4. Effect of oxygen concentration on degradation rate

The effect of external voltage, applied between the Ti/TiO<sub>2</sub> electrode and the Pt counter electrode, on the degradation rate of oxalic acid, was also investigated for three different oxygen concentrations of  $0.006$ ,  $6.7$  and  $27.9 \text{ mg dm}^{-3}$  at the light intensity of  $10.2 \times 10^{-5}$  einstein  $\text{m}^{-2} \text{s}^{-1}$ . The measured potentials of both Ti/TiO<sub>2</sub> and Pt electrode vs SCE are given in Table 3. Under open circuit conditions (i.e., without any applied potential), a negative  $E_{\text{Pt}}$  value of  $-0.39 \text{ V}$  was mea-

Table 3. Values of potentials of Ti/TiO<sub>2</sub> ( $E_{\text{Ti/TiO}_2}$ ) and Pt electrode ( $E_{\text{Pt}}$ ) vs SCE measured during degradation experiments at different oxygen concentrations and applied external voltage between Ti/TiO<sub>2</sub> and Pt electrode ( $E_{\text{Ti/TiO}_2}/(\text{vs Pt})$ )

$E_{\text{Ti/TiO}_2}(\text{vs Pt})$ /V	$\text{O}_2$ conc./ $\text{mg dm}^{-3}$					
	0.006		6.7		27.9	
	$E_{\text{Ti/TiO}_2}$ /V	$E_{\text{Pt}}$ /V	$E_{\text{Ti/TiO}_2}$ /V	$E_{\text{Pt}}$ /V	$E_{\text{Ti/TiO}_2}$ /V	$E_{\text{Pt}}$ /V
$E_{\text{oc}}$	-0.62	-0.39	-0.48	0.20	-0.39	0.19
0.0	-0.48	-0.49	-0.30	-0.30	-0.20	-0.19
0.5	-0.14	-0.66	0.13	-0.37	0.33	-0.18
1.0	0.31	-0.72	0.59	-0.41	0.80	-0.24
1.5	0.79	-0.73	1.04	-0.46	1.30	-0.24
2.0	1.40	-0.65	1.51	-0.49	1.81	-0.23

sured for the lowest oxygen concentration while positive  $E_{\text{Pt}}$  values of about  $+0.2 \text{ V}$  were measured for the oxygen concentrations of  $6.7$  and  $27.9 \text{ mg dm}^{-3}$ . It can be also seen in Table 3 that the  $E_{\text{Pt}}$  values decreased with the increasing external voltage as well as with the decreasing oxygen concentration. Due to the observed sensitivity of the  $E_{\text{Pt}}$  values to both applied voltage and oxygen concentration, the measured potential  $E_{\text{Ti/TiO}_2}$  (SCE) seems to be a more appropriate means for characterization of the external voltage effect than the actual value of the voltage between the Ti/TiO<sub>2</sub> electrode and the Pt counter electrode.

The dependencies of the degradation rate of oxalic acid on the Ti/TiO<sub>2</sub> potential (SCE) are shown in Figure 7, together with data for open circuit experiments. The degradation rate increased with increasing  $E_{\text{Ti/TiO}_2}$  values for all oxygen concentrations. The increase was most marked in the potential range from

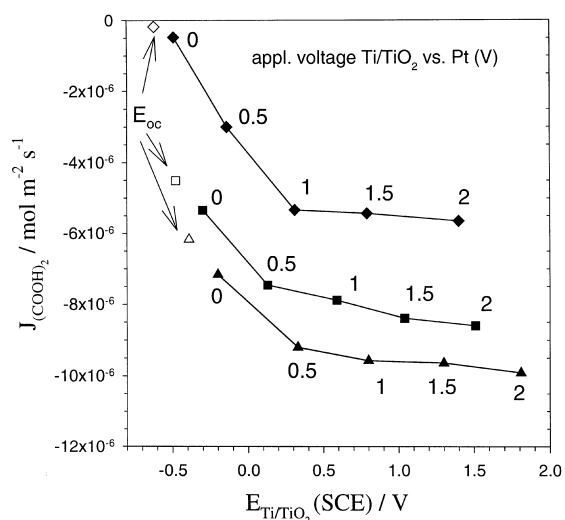


Fig. 7. Dependence of degradation rate of oxalic acid on Ti/TiO<sub>2</sub> potential (SCE) for three different bulk concentrations of oxygen (◆)  $0.006$ , (■)  $6.7$  and (▲)  $27.9 \text{ mg dm}^{-3}$   $J_{\text{hv}} = 10.2 \times 10^{-5}$  einstein  $\text{m}^{-2} \text{s}^{-1}$ , electrolyte  $0.1 \text{ M NaClO}_4$ , flow rate  $150 \text{ dm}^3 \text{ h}^{-1}$ , initial concentration of oxalic acid was  $0.005 \text{ M}$ .

–0.5 to about +0.4 V while it was more gradual for higher potentials.

At  $E_{oc}$  oxygen concentration  $0.006 \text{ mg dm}^{-3}$  the degradation rate is negligible but, when an external voltage of 1 V is applied, the degradation rate is comparable with that at  $E_{oc}$  at about three orders higher oxygen concentration ( $6.7 \text{ mg dm}^{-3}$ ). The finding that the degradation rate of oxalic acid with applied external voltage at almost zero oxygen concentration ( $0.006 \text{ mg dm}^{-3}$ ) is not negligible means, that instead of oxygen reduction, hydrogen evolution proceeded at the Pt counter electrode. This is consistent with the measured negative  $E_{Pt}$  value for the lowest oxygen concentration. The observed increase in the  $E_{Pt}$  values at higher oxygen concentrations corresponded with an increased participation of oxygen reduction in the overall reduction processes.

#### 4. Conclusions

- (i) Photocatalytic degradation of oxalic acid (initial concentration  $0.005 \text{ M}$ ) followed zero order kinetics.
- (ii) In the presence of oxalic acid the photocurrent increased by one order of magnitude.
- (iii) The degradation rate of oxalic acid increased with increasing potential of the Ti/TiO<sub>2</sub> electrode up to 0.5 V vs SCE then the decrease was much more gradual.
- (iv) Photogenerated electrons migrate from the illuminated Ti/TiO<sub>2</sub> electrode through the external circuit to the Pt counter electrode where, besides oxygen reduction, hydrogen evolution takes place. Therefore electrochemically assisted photocatalytic degradation of oxalic acid also proceeded in the absence of oxygen.

#### Acknowledgement

This work was supported by grant GA ĀR 203/99/0763 and 104/02/0662. The authors thank M. Heyrovský for helpful discussion during the development and preparation of this paper.

#### References

1. A. Fujishima and K. Honda, *Nature* **238** (1972) 37.
2. M. Gratzel, 'Heterogeneous Photochemical Electron Transfer' (CRC Press, 1989).
3. I.M. Butterfield, P.A. Christensen, A. Hamnett, K.E. Shaw, G.M. Walker and S.A. Walker, *J. Appl. Electrochem.* **27** (1997) 385.
4. L. Kavan and M. Grätzel, *Electrochim. Acta* **40** (1995) 643.
5. Y. Hamasaki, S. Ohkubo, K. Murakami, H. Sei and G. Nogami, *J. Electrochem. Soc.* **141** (1994) 660.
6. A. Hagfeldt, H. Lindstrom, S. Sodergren and S-E. Lindquist, *J. Electroanal. Chem.* **381** (1995) 39.
7. A. Shiga, A. Tsuiko, S. Yae and Y. Nakato, *Bull. Chem. Soc. Jpn.* **71** (1998) 2119.
8. D.H. Kim and M.A. Anderson, *Environ. Sci. Tech.* **28** (1994) 479.
9. J.K.N. Mbindyo, M.F. Ahmadi and J.F. Rusling, *J. Electrochem. Soc.* **144** (1997) 153.
10. P. Fernández-Ibáñez, S. Malato and O. Ernea, *Catal. Today* **54** (1999) 329.
11. K. Vinodgopal, S. Hotchandani and P.V. Kamat, *J. Phys. Chem.* **97** (1993) 9040.
12. K. Vinodgopal, U. Stafford, K.A. Gray and P.V. Kamat, *J. Phys. Chem.* **98** (1994) 6797.
13. J.A. Byrne and B.R. Eggins, *J. Electroanal. Chem.* **457** (1998) 61.
14. J.A. Byrne, B.R. Eggins, N.M.D. Brown, B. McKinney, M. Rouse, *Applied Catalysis B: Environmental* **17** (1998) 25.
15. J. Kulas, I. Roušar, J. Krýsa and J. Jirkovský, *J. Appl. Electrochem.* **28** (1998), 843.
16. J. Krýsa, L. Vodehnal and J. Jirkovský, *J. Appl. Electrochem.* **29** (1999), 429.
17. J. Krýsa, K. Bouzek and Ch. Stollberg, *J. Appl. Electrochem.* **30** (2000), 1033.
18. G. Dryhurst and D.L. McAllister, *Anal. Chim. Acta* **72** (1974), 209.